

# Development of poly(lactic acid)/ethylene-propylene-diene monomer/cellulose composites using cellulose extracted from hemp biomass for plastic packaging applications

Supanicha ALAPON<sup>1</sup>, Natthanich THONGMEE<sup>1</sup>, Wikoramet TEEKA<sup>1</sup>, Pattara SOMNUAKE<sup>1,2</sup>, and Sirirat WACHARAWICHANANT<sup>1,\*</sup>

#### Received date:

24 February 2025

#### Revised date:

11 June 2025

# Accepted date:

7 August 2025

# **Keywords:**

Poly(lactic acid); Ethylene-propylene-diene monomer (EPDM); Hemp biomass; Micro-cellulose;

# Abstract

Poly(lactic acid)/ethylene-propylene-diene monomer (EPDM)/cellulose composites using cellulose derived from hemp biomass (CHB) were investigated in this research. Morphology, chemical structures, functional groups, and crystallinity of CHB were characterized, observing a size of 135 ± 32 µm from SEM images with high purity and crystallinity from FT-IR and XRD spectroscopy. The optimized CHB was incorporated at 1 phr, 3 phr, and 5 phr into PLA/EPDM blends at 90/10 w/w. The polymer composites were prepared using an internal mixer, and samples were produced by compression molding for mechanical and thermal testing. The results indicated that the EPDM phase dispersed as droplets in the PLA matrix, resulting in more break elongation in the polymer blends from 3% to 9%. The CHB was not homogeneously distributed, with prominent particles observed in the matrix. Nevertheless, CHB enhanced Young's modulus, tensile strength, and stress at break, particularly in the 1 phr composites, which was identified as the optimal condition. The stress-strain curve shows the rigid shape of the neat material transforming to yield a point. For transparency, it shows that the EPDM and CHB mix resists UV and the visible range. Ultimately, the PLA/EPDM/CHB composites demonstrated improved properties suitable for plastic packaging applications.

# 1. Introduction

Polymer composites

Plastic pollution has emerged as one of the most pressing environmental challenges, representing a global ecological crisis that transcends geographical boundaries and affects all ecosystems. The nature of plastic contamination has reached alarming proportions, with plastic debris now detected in the deepest ocean trenches, highest mountain peaks, and even in human bloodstreams and placental tissues. Conservative estimates suggest that over 300 million tons of plastic waste are generated annually worldwide, with a significant portion entering natural environments where they persist for centuries. Conventional plastic bags, predominantly manufactured from petroleum-derived, non-biodegradable polymers, constitute a substantial fraction of this environmental problem [1-5].

The recognition of plastic pollution's devastating impacts has driven the scientific community and industry to explore biopolymers with inherent biodegradable properties as viable replacements for conventional plastics. Biodegradable polymers offer sound environmental degradation. Among the various biodegradable polymers under investigation, poly(lactic acid) (PLA) has emerged as one of the most promising alternative materials to replace petroleum-based counterparts [6]. PLA represents a unique class of thermoplastic aliphatic polyesters that can be synthesized from renewable biomass resources, primarily through the fermentation of agricultural feedstocks such as corn starch, sugarcane, cassava, and other carbohydrate-rich materials. The polymer exhibits excellent transparency, making it suitable for optical clarity applications. Its tensile strength and modulus are comparable to conventional plastics like polystyrene, while maintaining good thermal stability up to approximately 60°C to 70°C. These favorable processing properties enable PLA to be manufactured into various forms through conventional plastic processing techniques, including spinning into fibers for textile applications, casting into transparent films for packaging, extrusion for thermoformed containers, and injection molding for complex three-dimensional products [6-14].

While PLA offers excellent environmental credentials, its inherent brittleness and limited impact resistance can restrict its application in demanding end-uses that require enhanced toughness and flexibility. To address these limitations, polymer blending with elastomeric materials has emerged as an effective strategy to improve the mechanical performance. Ethylene-propylene-diene-monomer (EPDM) rubber is widely recognized as a high-performance synthetic elastomer. The synthetic composition of EPDM provides several practical advantages, including low manufacturing cost, extended shelf-life stability, excellent processability, and significantly enhanced elongation properties that can exceed 500% strain at break [15-18]. These characteristics make EPDM an attractive modifier for improving rigid thermoplastics' impact

<sup>&</sup>lt;sup>1</sup> Department of Chemical Engineering, Faculty of Engineering and Industrial Technology, Silpakorn University, Nakhon Pathom 73000,

<sup>&</sup>lt;sup>2</sup> School of Integrated Science and Innovation, Sirindhorn International Institute of Technology (SIIT), Thammasat University, Pathum Thani 12121, Thailand

<sup>\*</sup>Corresponding author e-mail: wacharawichanan s@su.ac.th

2 ALAPON, S., et al.

resistance and flexibility. In contrast to synthetic alternatives, natural rubber (NR) offers higher rates when exposed to appropriate environmental conditions, while synthetic rubber provides advantages in terms of prolonged shelf-life and enhanced polymer elasticity characteristics. The selection of rubber type must balance performance requirements with environmental impact considerations [18-21].

Hemp biomass, derived from the industrial hemp plant (Cannabis sativa L.), represents an up-and-coming source of natural reinforcing fibers for sustainable composite applications. Industrial hemp finds extensive utility across diverse industries, spanning traditional applications in textiles and cordage, modern construction materials including hemp-crate and insulation panels, biofuel production through biodiesel and bioethanol pathways, and nutritional health supplements derived from hemp seeds and extracts. The growing interest in hemp-derived cannabidiol (CBD) for pharmaceutical and wellness applications has created a substantial secondary benefit: the generation of significant quantities of post-extraction residual biomass. Following CBD extraction, the remaining hemp biomass emerges as a valuable by-product abundant in cellulose content, typically ranging from 40% to 60% by weight, depending on the plant variety and processing conditions. This high cellulose content makes hemp biomass ideal for utilization as a reinforcing fiber additive in composite materials, offering exceptional potential for value-added applications rather than disposal as agricultural waste [22-25]. As natural entities, cellulose fibers have attracted significant attention in composite material applications due to their unique combination of beneficial attributes. These include exceptional cost-effectiveness compared to synthetic reinforcing fibers, low density (typically 1.3 g·cm<sup>-3</sup> to 1.5 g·cm<sup>-3</sup>) which contributes to lightweight composite systems, considerable tensile strength (ranging from 300 MPa to 800 MPa depending on fiber source and treatment), excellent temperature resilience up to 200°C to 250°C before thermal degradation, and innate biodegradability that aligns with sustainable material development objectives. Hemp fibers, in particular, demonstrate exceptional lengthto-diameter ratios, good interfacial adhesion potential with polymer matrices, and favorable mechanical properties that make them competitive with traditional synthetic reinforcing materials [26, 27].

The primary aim of this research is to optimize the utilization of natural hemp fibers in developing composite materials. By systematically investigating the effects of hemp fiber incorporation into PLA-based polymer blends, the investigation formulated composite materials using a PLA matrix as the primary biodegradable polymer component. The polymer blend system incorporated EPDM rubber at a fixed concentration of 10% w/w to enhance toughness. Hemp biomass was added at 1 phr, 3 phr, and 5 phr concentrations to establish the relationship between fiber loading and resulting composite properties. The PLA/EPDM blends and CHB composites were processed using melt processing techniques, specifically designed to ensure uniform dispersion of the elastomeric modifier and natural fiber reinforcement throughout the polymer matrix. This processing approach enables the production of homogeneous composite materials suitable for subsequent characterization and potential commercial applications.

# 2. Experimental

### 2.1 Materials

Poly(lactic acid) (PLA) with a melt flow index of 6.0 g·min<sup>-1</sup> and a density of 1.24 g·cm<sup>-3</sup> was used in this research, and the commercial name is "Ingeo<sup>TM</sup> Biopolymer 2003D", produced by NatureWorks LLC, USA. EPDM with the ethylene content of 70.0 wt%, ethylidene norbomene (ENB) content of 0.5 wt%, and propylene content of 29.5 wt% was produced by Dow Chemical Company under the commercial name of "NORDEL<sup>TM</sup> IP 3745P", with the specific gravity of 0.88 g·cm<sup>-3</sup>. The hemp biomass (HB) was provided by Eastern Spectrum Group Co., Ltd, from the ethanol extraction by following the process: a centrifuge with ethanol at 40 °C to extract cannabidiol (CBD) and tetrahydrocannabinol (THC), classified as cannabinoids.

# 2.2 Preparation of cellulose from hemp biomass

The initial step involved removing oil from 20 g of hemp biomass through hexane extraction using a 1:10 biomass-to-solvent ratio at room temperature for 6 h. After that, the hemp biomass was separated using the vacuum pump and subsequently dried in an oven at 60°C for 24 h. The dried hemp biomass 20 g was stirred with NaOH 4 wt% at 80°C for 4 h. Then, wash with DI water. The bleaching process was completed using a ratio of 1:10 hydrogen peroxide (10%) at 80°C for 4 h. Last is acid hydrolysis using 10% hydrochloric acid at 60°C for 2 h. Thus, the samples were filtered and washed with DI water in the chemical treatments until the products were neutral. Lastly, it is dried in an oven at 60°C for 24 h.

# 2.3 Sample preparation

Polymers and cellulose were dried at 80°C for 4 h before mixing. EPDM does not need to be dry. PLA was dried in an oven at 80°C for 4 h, and CHB at 80°C for 24 h. Initially, PLA and PLA/EPDM blends were prepared in an internal mixer at 170°C and a rotor speed of 50 rpm for 15 min. CHB was added 3 min of blending, where the mixing was performed. PLA/CHB composites were used under the same conditions. Afterward, the neat polymer, the polymer blends, and the polymer composites were compressed into standard dumbbell tensile bars at 170°C for 10 min for further tensile testing. The film was formed using a temperature of 170°C for 5 min in a compression molding.

# 2.4 Sample characterization

The tensile testing of neat PLA and PLA/EPDM blends and PLA/EPDM/CHB composites was measured using a universal testing machine (EZ Test, EZ-LX/EZ-SX Series) at a crosshead speed of 50 mm·min<sup>-1</sup>; each value obtained represented the average of five samples. Microcellulose and break-fractured polymer surface morphology was observed using Scanning Electron Microscopy (SEM, TESCAN MIRA3). The functional groups of cellulose from hemp biomass (CHB) were investigated by Fourier Transform Infrared (FT-IR) Spectroscopy. Polymer blends and composites were analyzed by TGA (STD Q600) to study the thermal stability. Thermal behavior was studied by using a DSC (STD Q600). The percent crystallinity of polymers was calculated by

$$\%X_c = \frac{\Delta H_m - \Delta H_c}{\Delta H m_0} \times 100 \tag{1}$$

where is  $\Delta Hm$  the enthalpy of sample melting,  $\Delta Hc$  is the enthalpy of crystallization,  $\Delta Hm0$  is the 100% crystals melting enthalpy ( $\Delta Hm0$  of PLA is 93.7 J·g<sup>-1</sup>) [7, 28]. The investigation film's UV-Vis blocking properties and absorbency were recorded in the 200 nm to 800 nm range using a UV-Vis spectrophotometer (VARIAN, Cary 5000).

#### 3. Results and discussion

# 3.1 Morphology and chemical structures of cellulose from hemp biomass (CHB)

SEM characterized the morphology of cellulose from hemp biomass (CHB) at magnification 150x to estimate the size of the cellulose and at magnification 2000x to observe the surface morphology, as shown in Figure 1. The fiber length, about  $135 \pm 32 \mu m$ , is shown in Figure 1(a), which in the red outline. The other components of hemicellulose and a small amount of lignin on the CHB fiber core structure are zoomed in and shown in Figure 1(b) [29]. It can indicate that the lignin and hemicellulose of the substance still exist in small amounts, although it passes the extraction. It can be supported by FT-IR spectroscopy, which was used to analyze the functional group analysis of different solution-treated CHB structures as shown in Figure 2(a). The peak at 3333 cm<sup>-1</sup> is the stretch vibration peak of the OH group. The prominent peaks at 2915 cm<sup>-1</sup> and 2848 cm<sup>-1</sup> are caused by stretching vibrations of the CH group. The peak at  $1624~\text{cm}^{-1}$  is the stretching of the C=O bond, which is the vibration of the carboxyl group in hemicellulose. Moreover, the peak at 1425 cm<sup>-1</sup> shows the flexion vibration of CH<sub>2</sub> and the CH peak of lignin. The peak at 1162 cm<sup>-1</sup> bond is formed by the elongation of -C-O-C- symmetric stretching [30], an ester compound, where NaOH hydrolyzes the ester in the lignin molecule, causing hemicellulose to be cleaved. The peak at 1162 cm<sup>-1</sup> was reduced more than the bond of hexane, indicating that hemicellulose could be extracted by sodium hydroxide [31] while reaching the peak at 1020 cm<sup>-1</sup> of CHB [32]. As other peaks decrease, we can remove other unwanted substances in CHB, and the peak of 872 cm<sup>-1</sup> is attributed to the stretching vibrations of the C–O bond from the polyester [33].

#### 3.2 Characterization of polymer blend and composites

The X-ray diffraction (XRD) analysis reveals significant structural changes following the alkali-acid treatment of raw hemp fibers, as shown in Figure 2(b). From other works, the XRD pattern of the cellulose standard shows diffraction peaks at 14°, 16.5°, and 22.5°, characteristic of the crystalline form of cellulose [34]. The raw hemp exhibits a predominantly amorphous character with broad, lowintensity reflections and considerable baseline noise, indicating the presence of lignin, hemicellulose, and other non-cellulosic components contributing to the structural disorder. In contrast, CHB displays sharp, well-defined crystalline peaks characteristic of cellulose I structure, with prominent reflections at approximately  $16^{\circ}$  and  $22^{\circ}\,2\theta$  corresponding to the (110) and (200) crystallographic planes, respectively [23,35-39]. These planes represent the lateral packing arrangements of cellulose chains within the crystal matrix, where the (200) plane (d-spacing ~3.9 Å to 4.0 Å) reflects inter-chain spacing perpendicular to the a-axis, and the (110) plane (d-spacing ~5.4 Å to 6.0 Å) represents the crosssectional arrangement of parallel cellulose chains. The peak positions at 20° and 26.5° may indicate either a different cellulose polymorph, as possibly cellulose II formed during the alkali treatment, lattice

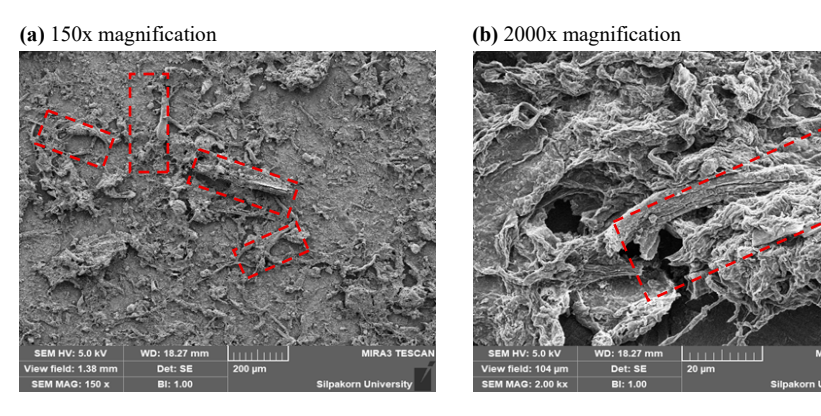


Figure 1. SEM micrographs of cellulose from hemp biomass (CHB) after acid hydrolysis with hydrochloric acid.

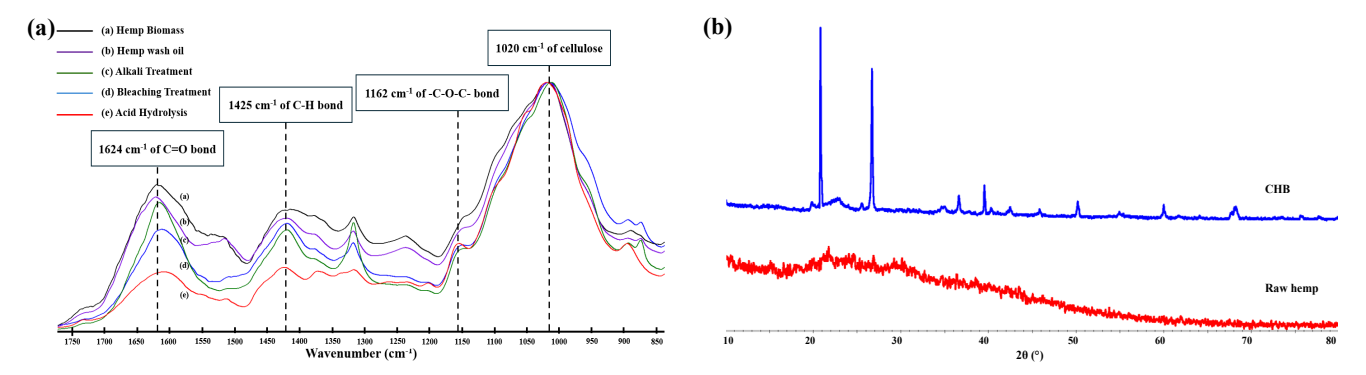


Figure 2. FT-IR spectra of cellulose from hemp biomass (a) and XRD traces of cellulose from hemp biomass (b).

strain, or require proper indexing against cellulose crystal structure databases for accurate Miller indices assignment. The NaOH, H<sub>2</sub>O<sub>2</sub>, and HCl treatment successfully removed amorphous matrix materials while creating a highly crystalline cellulose structure. This resulted in a significantly improved crystallinity index and confirmed the effective purification of the raw hemp biomass. In conclusion, the SEM surface morphology, FT-IR spectroscopy, and XRD analysis support that the CHB is a micron-sized, high-purity, and highly crystalline cellulose, which can be used as a composite to increase the polymer properties [33].

# 3.2.1 Morphology

The SEM micrographs of neat PLA, PLA/EPDM blends, and CHB composites 1 phr, 3 phr, and 5 phr were observed and investigated. Firstly, the fracture surfaces of neat PLA and the fracture surface of PLA/CHB are shown in Figure 3(a-d). The neat PLA surface was smooth due to the properties of the material. After adding CHB is still a rigid fracture, but does not have smooth surfaces. The average size of CHB particles in the PLA matrix was about  $132 \pm 38~\mu m$ . After mixing in the PLA matrix, the CHB did not have a different particle size.

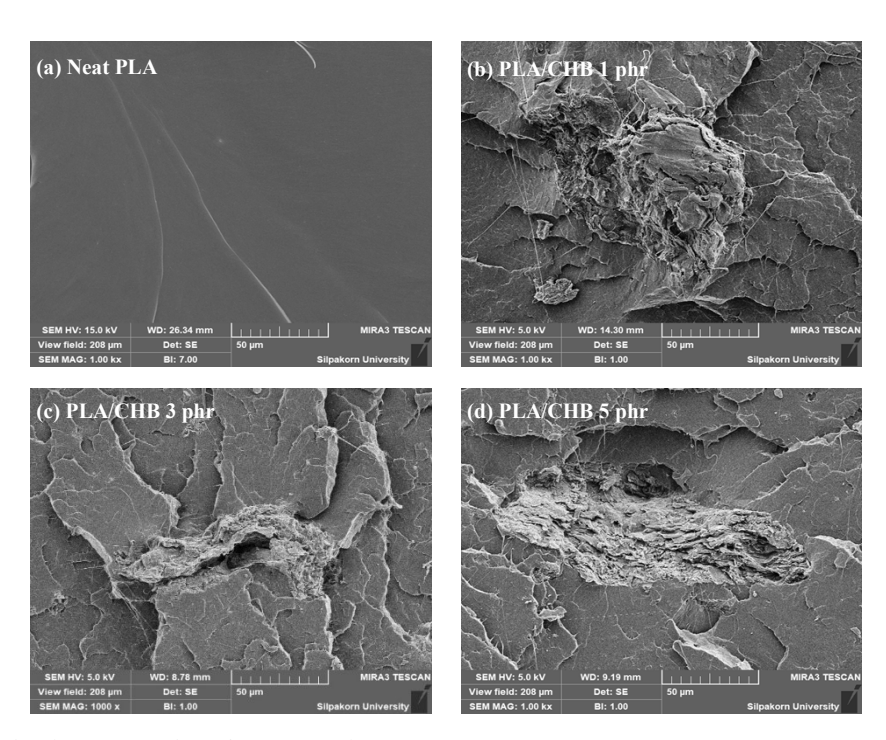


Figure 3. SEM micrographs of neat PLA and PLA/CHB composites.

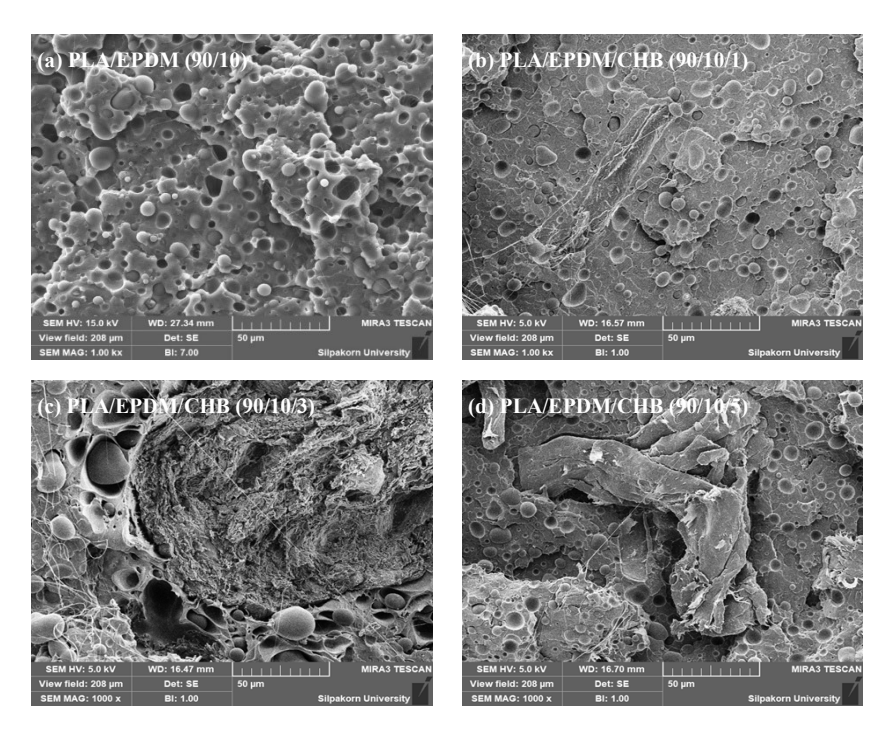


Figure 4. SEM micrographs of PLA/EPDM/CHB composites.

The fracture surface of PLA/EPDM/CHB composites is shown in Figure 4(b-d). The fracture is rough and complicated, so it should be more elongated. Not only that, considering the grain size and particle size mixed in the PLA matrix, the grain size of PLA/EPDM blends was about 6 µm, which is small. The average grain size of EPDM compounds was about 8 µm. The rubber granules in the PLA matrix provide a larger granule size than PLA/EPDM blends [40]. In terms of CHB, it can be seen that the CHB is still the big particle in the polymer blends. It can be described that the polymer blends and internal mixer do not affect the decrease in the size of the cellulose [27,41]. Others' work confirms the droplet feature of EPDM, which is the same as this work, both in observation and in the size of its droplet, for more confirmation of component matching [38]. In a part of cellulose, the SEM-EDS was used to confirm by using the different ratios of elements from the periodic table. Cellulose feature with high Oxygen illustrated with the fiber feature in the blue area [34].

# 3.2.2 Mechanical properties

The tensile stress-strain curves of PLA, PLA/EPDM, PLA/CHB, and PLA/EPDM/CHB are shown in Figure 6. The results of the neat PLA showed low mechanical properties. After adding the elastomer, the PLA/EPDM (90/10) shows the highest break elongation improvement. It indicated that PLA was toughened by EPDM, which corresponded with the roughness of the fracture surface morphology. On the other hand, adding CHB increases the tensile strength and Young's modulus of PLA, but those at 1 phr, and 3 phr composites significantly increase compared to the 5 phr for CHB addition. It can be from the CHB agglomerated in the PLA matrix, which is too much added into the polymer [19,42]. The shape of the stress-strain curves of neat PLA and PLA/CHB shows

the same configuration: a sharp curve with high stress and low strain. It is the shape of a rigid material. Then, PLA/EPDM and PLA/EPDM/ CHB 1 phr show that the materials can maintain the force after passing the yield point. It can be confirmed that the PLA/EPDM/CHB 1 phr is a more stable material, although the PLA/EPDM blended shows a higher elongation at break. It indicates that the CHB in an approximate ratio can improve the force stability of the material. However, adding 3 phr and 5 phr of CHB decreased for all properties. It can be from the separate phase of CHB, which is too much [7,19,43].

The mechanical and tensile testing results are summarized and shown in Table 1. Neat PLA shows a high Young's modulus but low tensile strength and elongation at break. The PLA/EPDM blends showed a significant increase in elongation at break, but Young's modulus, tensile strength, and stress at break decreased from those of the neat PLA. The results showed that the EPDM blend can solve the brittleness of PLA [44]. The CHB addition increases tensile strength, especially for 1 phr, and 3 phr, which indicates that the CHB acts as a reinforced fiber for the PLA matrix. Not only that, but the stress at break and modulus also increased from the neat, which means that the CHB improves the mechanical strength and rigidity of the polymer. After balancing elastic and reinforcement, CHB addition shows the improvement of Young's modulus from PLA/EPDM blended, but not close to neat PLA, except at 5 phr of CHB composited, which increased slightly as neat PLA. Adding hemp biomass at 5 phr decreased the elongation, which was inconsistent with the objective of this research. Therefore, CHB was determined at 1 phr. Young's modulus was increased from the neat, and the elongation was higher. Also, the force of the curves is stable and not too rigid in shape. It can be concluded that the CHB addition at 1 phr in PLA/EPDM is the optimum ratio to apply for plastic packaging applications [7].



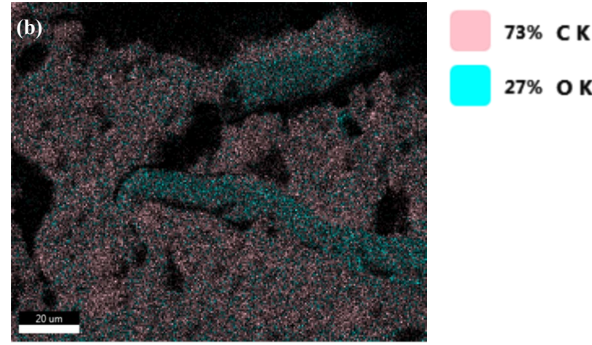
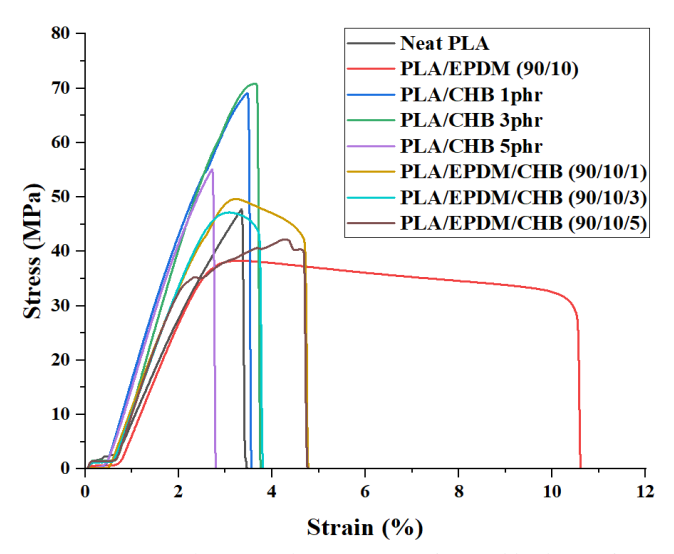


Figure 5. SEM micrographs (a), and EDS (b) of PLA/EPDM/CHB composites.

Table 1. Summary of comparison of mechanical properties of neat PLA, PLA/EPDM blends, PLA/CHB, and PLA/EPDM/CHB composites.

Sample	Young's modulus	Tensile strength	Stress at break	Elongation at break	
	[MPa]	[MPa]	[MPa]	[%]	
Neat PLA	$2231.7 \pm 243.4$	$42.7 \pm 4.7$	$42.9 \pm 4.8$	$3.5 \pm 0.5$	
PLA/EPDM (90/10)	$2105.7 \pm 10.1$	$19.6 \pm 1.4$	$30.9 \pm 5.0$	$9.1 \pm 2.0$	
PLA/CHB 1 phr	$2920.6 \pm 69.2$	$69.2 \pm 1.7$	$69.1 \pm 1.7$	$3.6 \pm 0.5$	
PLA/CHB 3 phr	$3059.6 \pm 22.2$	$69.5 \pm 1.2$	$69.5 \pm 1.2$	$3.5 \pm 0.1$	
PLA/CHB 5 phr	$2954.5 \pm 86.9$	$59.4 \pm 4.4$	$59.4 \pm 4.4$	$2.9 \pm 0.3$	
PLA/EPDM/CHB (90/10/1)	$2346.8 \pm 66.2$	$48.5\pm1.2$	$40.7 \pm 5.5$	$4.8\pm1.3$	
PLA/EPDM/CHB (90/10/3)	$2389.8 \pm 12.1$	$47.7 \pm 0.5$	$45.1\pm0.8$	$5.1 \pm 1.3$	
PLA/EPDM/CHB (90/10/5)	$2529.0 \pm 28.9$	$43.4 \pm 7.3$	$45.1 \pm 4.5$	$3.7 \pm 1.0$	

6 ALAPON, S., et al.



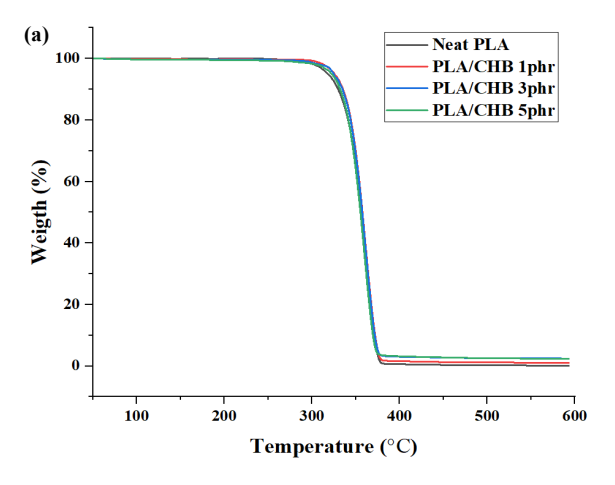
**Figure 6.** Stress-strain curves of neat PLA, PLA/EPDM blends, PLA/CHB composites, and PLA/EPDM/CHB composites.

# 3.2.3 Thermal properties

The thermal properties of PLA blends and composites were investigated and recorded in Table 2.  $T_g$ ,  $T_c$ , and  $T_m$  of polymer blends and composites do not significantly influence, which can be described as the quality of the crystalline and the form of the amorphous phases do not change [45-47]. In terms of the quality of crystallinity, the percent

crystallinity (%Xc) is calculated from the enthalpy of crystallization ( $\Delta$ Hc) and enthalpy of melting ( $\Delta$ Hm). Co-crystallization of the PLA matrix is almost unaffected by adding CHB. However, EPDM rubber is significantly affected by DSC crystallinity. It can increase to about 10% crystallinity compared to neat PLA. After adding the CHB to polymer blends, the crystallinity percentage decreased when more CHB was added to the polymer blends. The disruption of CHB will make crystallization in polymers harder [7,18]. Overall, the EPDM blends show increased crystallinity, but after adding CHB, the crystallinity cannot be formed without change at all temperatures.

Thermal degradation behavior from TGA analysis of PLA and PLA/CHB is shown in Figure 7(a). The initial decomposition temperature depends on the additive in polymer blends and composites. Slightly higher yields for composite mats persist because CHB is more stable in the temperature range above 310°C than neat PLA. CHB composites show a somewhat lower weight loss than PLA/CHB below 300°C, where the mixture of CHB increased with a ratio that did not affect degradation. PLA/EPDM exhibits a two-step degradation pattern of about 300°C to 600°C, as shown in Figure 7(b). The first and second degradation steps in the polymer blends corresponded to the degradation of PLA and EPDM, respectively. The thermal stability of the PLA/EPDM polymer blend decreased after adding CHB with an increased ratio of CHB [28]. It can be concluded that the CHB is more stabilized than the PLA, but still has lower properties than the EPDM rubber. It is another reason for using synthetic rubber in materials [5,6].



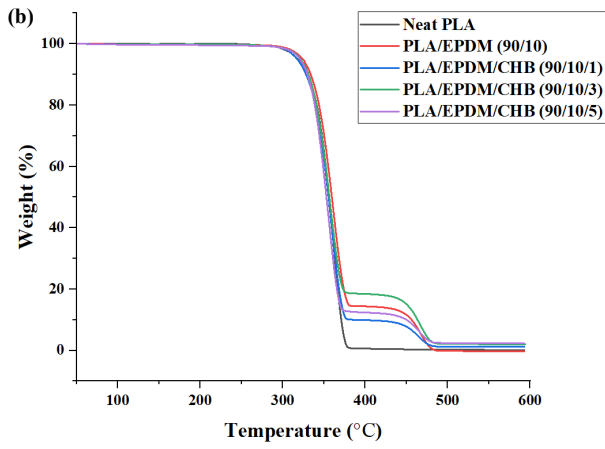


Figure 7. TGA thermograms diffraction of PLA/CHB (a) and PLA/EPDM/CHB composites (b).

Table 2. Thermal properties and %crystallinity of neat PLA, PLA/EPDM blend, PLA/CHB, and PLA/EPDM/CHB composites.

Sample	Tg	T <sub>c</sub>	T <sub>m</sub>	$\Delta \mathbf{H_c}$	$\Delta \mathbf{H}_{\mathbf{m}}$	Crystallinity T <sub>d10</sub> T <sub>d50</sub>		$T_{d50}$
	[°C]	[°C]	[°C]	[ <b>J</b> ⋅ <b>g</b> <sup>-1</sup> °C]	[ <b>J</b> ⋅ <b>g</b> <sup>-1</sup> ° <b>C</b> ]	[%]	[°C]	[°C]
Neat PLA	63	122	153	33.1	38.3	5.5	330	360
PLA/EPDM (90/10)	62	117	154	30.1	43.1	13.9	334	360
PLA/CHB 1 phr	59	118	150	118.0	149.9	1.2	335	357
PLA/CHB 3 phr	59	118	151	120.5	150.2	0.3	335	357
PLA/CHB 5 phr	60	116	151	117.0	149.9	1.2	332	355
PLA/EPDM/CHB (90/10/1)	60	117	151	117.5	150.2	2.0	328	357
PLA/EPDM/CHB (90/10/3)	61	119	152	120.2	151.2	0.7	331	357
PLA/EPDM/CHB (90/10/5)	60	120	151	120.5	151.0	1.2	330	353

# 3.2.4 Crystallinity

XRD analysis is the main characterization used to investigate the crystallization. Thus, the result of XRD is demonstrated in Figure 8. Neat PLA exhibits broad diffraction peaks with maximum intensity at  $2\theta = 15^{\circ}$  with no crystalline peaks, as shown in Figure 8(a). Because of the fast-cooling step, the melting process with the internal mixer and compression molding took no time to generate crystal formation. Regarding EPDM rubber in Figure 8(b), it also shows a broad peak like PLA, but at a different position at  $2\theta = 20^{\circ}$  and a tiny peak at  $28^{\circ}$ . Although both materials show almost broad amorphous regions, the PLA was amorphous from the processing, while the EPDM was amorphous by nature of rubber [48]. After blending, PLA/EPDM shows the amorphous region, but it looks like it combines the PLA and EPDM features, as illustrated in Figure 8(c). It has some small peaks from EPDM at 28°, which do not affect all the crystals because of the too small amount. It can be confirmed that the materials were blended without generating more crystal formation. The PLA/EPDM/ CHB composites at 1 phr, 3 phr, and 5 phr, as shown in Figure 8(e-f), show few crystallizations observed at 20° and an intense peak, which follows the trends at 26.5°, consistent with the band from CHB. Moreover, at 28°, EPDM still aligns. Although both showed a strong band in neat CHB, they show a low intensity after mixing with polymers at 20°. It is because the broad peak of both polymers overlays the CHB feature. Lastly, CHB and EPDM were not affected too much in crystallization because the heat process is a core factor affecting the crystallinity. However, it still helps in mechanical and optical properties for the applications [49-51].

# 3.2.5 Optical properties

UV-Vis absorption spectra of neat PLA and its composites are shown in Figure 9(a). Neat PLA showed the highest transmission in the visible region of the spectra (400 nm to 700 nm), and the PLA/CHB composites show a transmission-blocking at the UV spectra region (250 nm to 400 nm) [41]. This is because the transmission region of PLA was performed, but after CHB was added to the matrix, CHB protected the light before it passed the material sheet. Figure 9(b) shows the high absorption from EPDM after being added to the PLA matrix. The EPDM is a cloudy material that can protect against UV and visible light. After adding CHB to polymer blends, it was found that the increase of CHB contributed to improving the light absorption, respectively, with UV-Vis spectra showing the transmittance of PLA that was higher than that of PLA/CHB. It can be concluded that adding CHB can absorb the light better than neat PLA, including PLA/EPDM, at a ratio of 90/10. It positively affects light protection applications in plastic packaging. The light-blocking properties of the application will make the packaged items last longer and longer by preventing light from passing through [33,52].

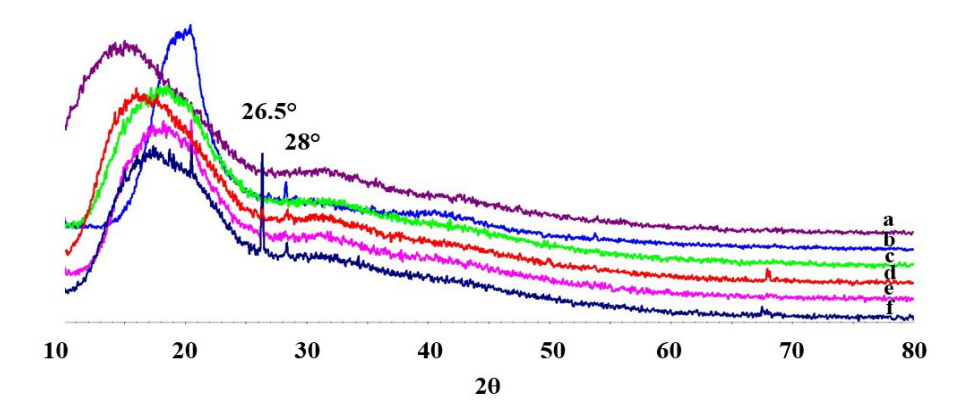


Figure 8. XRD diffraction patterns of neat PLA (a), neat EPDM (b), PLA/EPDM (c), and PLA/EPDM/CHB at 1 phr, 3 phr, and 5 phr (d-f) composites.

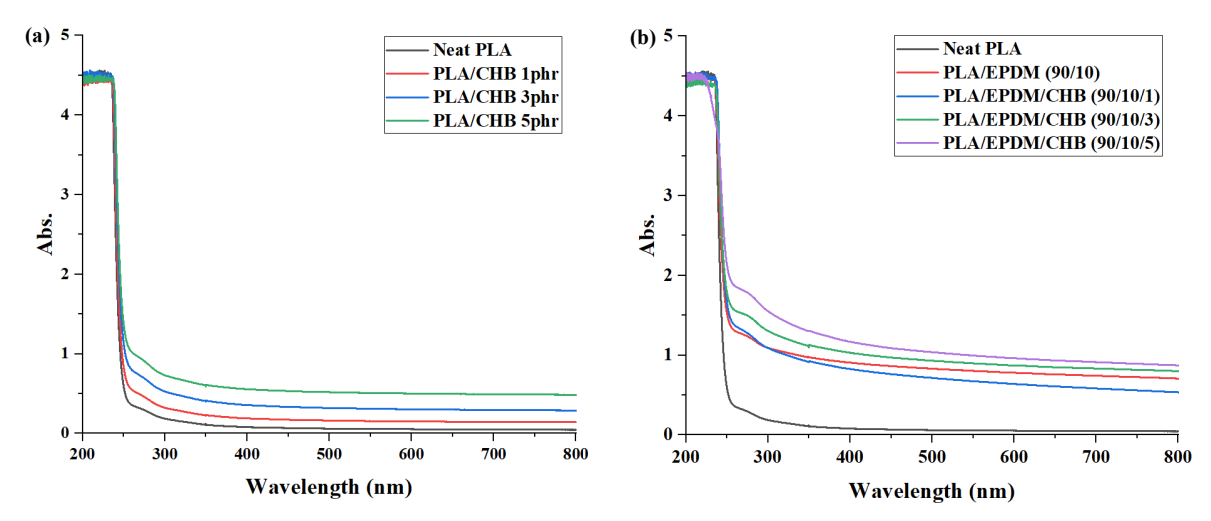


Figure 9. UV-vis absorption spectroscopy of PLA/CHB (a) and (b) PLA/EPDM/CHB composites.

# 4. Conclusions

This work aimed to extract CHB as an additive to improve the properties of plastic packaging applications. FT-IR revealed that hemicellulose and lignin can be removed, which results in parallel FT-IR evaluations, in which the number of substances to be removed is reduced, which suggests that micro-cellulose can be extracted from hemp biomass. Regarding polymer blends and composites, the best sequence mixing of polymer blends is PLA/EPDM, adding CHB 1 phr because it has the highest mechanical properties. There was also no significant change in thermal properties with another sequence mixing, although the degree of crystallinity was unequal. Therefore, EPDM was mixed at a ratio of 10 wt% to improve elongation properties at the break because of the plastic packaging. However, the best ratio of PLA/EPDM/CHB is 1 phr composites because it is more rigid and flexible when compared with other ratios. This is because the ratio of PLA/EPDM/CHB (90/10/1) composites has mechanical properties similar to bio-plastic glass; while plastic bags can be made, products can also be made. Moreover, this condition shows the high UV-Vis transmittance. Lastly, the CHB was synthesized and value-added with the PLA/EPDM/CHB (90/10/1), which provides the best application to bio-packaging materials.

# Acknowledgements

This research is financially supported by Thailand Science Research and Innovation (TSRI) National Science, Research and Innovation Fund (NSRF) (Fiscal Year 2024). The authors gratefully acknowledge Professor Dr.Piyasan Praserthdam, a Center of Excellence on Catalysis and Catalytic Reaction Engineering member, Department of Chemical Engineering, Faculty of Engineering, Chulalongkorn University, for any characterization equipment support and Eastern Spectrum Group Co., Ltd for supporting the hemp biomass used in this research.

# References

- [1] W. L. Filho, U. Saari, M. Fedoruk, A. Iital, H. Moora, M. Kloga, and V. Voronova, "An overview of the problems posed by plastic products and the role of extended producer responsibility in Europe," *Journal of cleaner production*, vol. 214, pp. 550-558, 2019.
- [2] P. Europe, "Plastics—The Facts 2016," *An analysis of European latest plastics production, demand and waste data,* 2016.
- [3] S. Buaruk, P. Somnuake, S. Gulyanon, S. Deepaisarn, S. Laitrakun, and P. Opaprakasit, "Membrane filter removal in FTIR spectra through dictionary learning for exploring explainable environmental microplastic analysis," *Scientific Reports*, vol. 14, no. 1, p. 20297, 2024.
- [4] S. Ebnesajjad, Fluoroplastics, volume 2: Melt processible fluoropolymers-the definitive user's guide and data book. William Andrew, 2015.
- [5] L. Cabernard, L. Roscher, C. Lorenz, G. Gerdts, and S. Primpke, "Comparison of Raman and Fourier transform infrared spectroscopy for the quantification of microplastics in the aquatic environment,"

- *Environmental science & technology*, vol. 52, no. 22, pp. 13279-13288, 2018.
- [6] P. Somnuake, P. Opaprakasit, and A. Petchsuk, "Electrospun nanofibers of polylactide (PLA) stereocomplex with superhydrophobic surfaces for potential use in facial mask and biomedical applications," Thammasat University, 2021.
- [7] A. Awal, M. Rana, and M. Sain, "Thermorheological and mechanical properties of cellulose reinforced PLA bio-composites," *Mechanics of Materials*, vol. 80, pp. 87-95, 2015.
- [8] T. C. Mokhena, J. S. Sefadi, E. R. Sadiku, M. J. John, M. J. Mochane, and A. Mtibe, "Thermoplastic processing of pla/cellulose nanomaterials composites," *Polymers (Basel)*, vol. 10, no. 12, 2018.
- [9] J. Ren, "Processing of PLA," in Biodegradable Poly(Lactic Acid): Synthesis, Modification, Processing and Applications. Berlin, Heidelberg: Springer Berlin Heidelberg, 2010, pp. 142-207.
- [10] S. Su, R. Kopitzky, S. Tolga, and S. Kabasci, "Polylactide (PLA) and its blends with poly(butylene succinate) (PBS): A brief review," *Polymers (Basel)*, vol. 11, no. 7, 2019.
- [11] X. Pang, X. Zhuang, Z. Tang, and X. Chen, "Polylactic acid (PLA): Research, development and industrialization," *Biotechnology Journal*, vol. 5, no. 11, pp. 1125-1136, 2010.
- [12] S. Li, S. Zhao, Y. Hou, G. Chen, Y. Chen, and Z. Zhang, "Polylactic acid (PLA) modified by polyethylene glycol (PEG) for the immobilization of lipase," *Applied biochemistry and biotechnology*, vol. 190, pp. 982-996, 2020.
- [13] H. Tsuji, "Poly(lactic acid) stereocomplexes: A decade of progress," *Advanced Drug Delivery Reviews*, vol. 107, pp. 97-135, 2016.
- [14] K. Madhavan Nampoothiri, N. R. Nair, and R. P. John, "An overview of the recent developments in polylactide (PLA) research," *Bioresour Technol*, vol. 101, no. 22, pp. 8493-501, 2010.
- [15] I. Reinholds, V. Kalkis, J. Zicans, R. Merijs Meri, and A. Grigalovica, "Thermal and mechanical properties of unvulcanized polypropylene blends with different elastomers: ethylene-propylene-diene terpolymer, nitrile-butadiene copolymer and chlorinated polyethylene," *Key Engineering Materials*, vol. 559, pp. 93-98, 2013.
- [16] P. Sukpuang, M. Opaprakasit, A. Petchsuk, and P. Opaprakasit, "Toughness enhancement of polylactic acid by employing glycolyzed polylactic acid-cured epoxidized natural rubber," in *Advanced Materials Research*, vol. 1025, pp. 580-584, 2014.
- [17] S. Wang, S. Pang, L. Pan, N. Xu, H. Huang, and T. Li, "Compatibilization of poly(lactic acid)/ethylene-propylenediene rubber blends by using organic montmorillonite as a compatibilizer," *Journal of Applied Polymer Science*, vol. 133, no. 46, 2016.
- [18] A. Piontek, O. Vernaez, and S. Kabasci, "Compatibilization of poly (lactic acid)(PLA) and bio-based ethylene-propylenediene-rubber (EPDM) via reactive extrusion with different coagents," *Polymers*, vol. 12, no. 3, p. 605, 2020.
- [19] Y.-X. Wang, C.-C. Wang, Y. Shi, L.-Z. Liu, N. Bai, and L.-F. Song, "Effects of dynamic crosslinking on crystallization,

- structure and mechanical property of ethylene-octene elastomer/ EPDM blends," *Polymers*, vol. 14, no. 1, p. 139, 2021.
- [20] J. Zhao, G. Wang, J. Chai, E. Chang, S. Wang, A. Zhang, and C. B. Park, "Polylactic acid/UV-crosslinked in-situ ethylenepropylene-diene terpolymer nanofibril composites with outstanding mechanical and foaming performance," *Chemical Engineering Journal*, vol. 447, p. 137509, 2022.
- [21] L. Wongwad, and S. Wacharawichanant, "Development of poly (lactic acid) ternary blends properties for plastic packaging applications by thermoforming technique," Silpakorn University, 2022.
- [22] S. Beluns, S. Gaidukovs, O. Platnieks, G. Gaidukova, I. Mierina, L. Grase, O. Starkova, P. Brazdausks, and V. K. Thakur, "From wood and hemp biomass wastes to sustainable nanocellulose foams," *Industrial Crops and Products*, vol. 170, p. 113780, 2021.
- [23] L. Lawson, L. M. Degenstein, B. Bates, W. Chute, D. King, and P. I. Dolez, "Cellulose textiles from hemp biomass: Opportunities and challenges," *Sustainability*, vol. 14, no. 22, p. 15337, 2022.
- [24] R. Sausserde, and A. Adamovics, "Industrial hemp for biomass production," *Journal of Agricultural Engineering*, vol. 44, no. s2, 2013.
- [25] J. Zhao, Y. Xu, W. Wang, J. Griffin, K. Roozeboom, and D. Wang, "Bioconversion of industrial hemp biomass for bioethanol production: A review," *Fuel*, vol. 281, p. 118725, 2020.
- [26] J. W. Dunlop, and P. Fratzl, "Biological composites," *Annual Review of Materials Research*, vol. 40, pp. 1-24, 2010.
- [27] B. E. Arteaga-Ballesteros, A. Guevara-Morales, E. S. Martín-Martínez, U. Figueroa-López, and H. Vieyra, "Composite of polylactic acid and microcellulose from kombucha membranes," e-Polymers, vol. 21, no. 1, pp. 015-026, 2020.
- [28] A. K. Mohapatra, S. Mohanty, and S. K. Nayak, "Properties and characterization of biodegradable poly (lactic acid)(PLA)/poly (ethylene glycol)(PEG) and PLA/PEG/organoclay: A study of crystallization kinetics, rheology, and compostability," *Journal* of Thermoplastic Composite Materials, vol. 29, no. 4, pp. 443-463, 2016.
- [29] X. Yang, L. Li, W. Zhao, M. Wang, W. Yang, Y. Tian, R. Zheng, S. Deng, Y. Mu, and X. Zhu, "Characteristics and functional application of cellulose fibers extracted from cow dung wastes," *Materials*, vol. 16, no. 2, p. 648, 2023.
- [30] B. Abderrahim, E. Abderrahman, A. Mohamed, T. Fatima, T. Abdesselam, and O. Krim, "Kinetic thermal degradation of cellulose, polybutylene succinate and a green composite: comparative study," *World Journal of Environmental Engineering*, vol. 3, no. 4, pp. 95-110, 2015.
- [31] V. Andritsou, E. M. de Melo, E. Tsouko, D. Ladakis, S. Maragkoudaki, A. A. Koutinas, and A. Matharu, "Synthesis and characterization of bacterial cellulose from citrus-based sustainable resources," ACS omega, vol. 3, no. 8, pp. 10365-10373, 2018.
- [32] M. Ibrahim, O. Osman, and A. A. Mahmoud, "Spectroscopic analyses of cellulose and chitosan: FTIR and modeling approach," *Journal of Computational and Theoretical Nanoscience*, vol. 8, no. 1, pp. 117-123, 2011.

- [33] R. Javier-Astete, J. Jimenez-Davalos, and G. Zolla, "Determination of hemicellulose, cellulose, holocellulose and lignin content using FTIR in calycophyllum spruceanum (Benth.) K. Schum. and Guazuma crinita Lam," *PLoS One*, vol. 16, no. 10, p. e0256559, 2021.
- [34] H. K. Lim, H. Y. Song, J. H. Ko, S. A. Lee, K.-I. Lee, and I. T. Hwang, "An alternative path for the preparation of triacetylcellulose from unrefined biomass," *Advances in Chemical Engineering and Science*, vol. 5, no. 1, pp. 33-42, 2014.
- [35] J. Zhang, Y. Wang, L. Zhang, R. Zhang, G. Liu, and G. Cheng, "Understanding changes in cellulose crystalline structure of lignocellulosic biomass during ionic liquid pretreatment by XRD," *Bioresource technology*, vol. 151, pp. 402-405, 2014.
- [36] K. Piekarska, P. Sowinski, E. Piorkowska, M. M. U. Haque, and M. Pracella, "Structure and properties of hybrid PLA nanocomposites with inorganic nanofillers and cellulose fibers," *Composites Part A: Applied Science and Manufacturing*, vol. 82, pp. 34-41, 2016.
- [37] R. Liu, H. Yu, and Y. Huang, "Structure and morphology of cellulose in wheat straw," *Cellulose*, vol. 12, pp. 25-34, 2005.
- [38] P. Somnuake, P. Puttawong, and S. Wacharawichanant, "Morphology and properties of poly(lactic acid)/ethylene propylene diene monomer blends with micro-cellulose fibers from paper pulp," *Advances in Science and Technology*, vol. 150, pp. 3-10, 2024.
- [39] R. Rotaru, M. Savin, N. Tudorachi, C. Peptu, P. Samoila, L. Sacarescu, and V. Harabagiu, "Ferromagnetic iron oxide–cellulose nanocomposites prepared by ultrasonication," *Polymer Chemistry*, vol. 9, no. 7, pp. 860-868, 2018.
- [40] A. Sowińska, M. Maciejewska, L. Guo, and E. Delebecq, "Task-specific ionic liquids with lactate anion applied to improve ZnO dispersibility in the ethylene-propylene-diene elastomer," *Polymers*, vol. 13, no. 5, p. 774, 2021.
- [41] E. Elisabeta, M. Rapa, O. Popa, G. Mustatea, V. L. Popa, A. Mitelut, and M. E. Popa, "Polylactic acid/cellulose fibres based composites for food packaging applications," *Materiale Plastice*, vol. 54, no. 4, pp. 673-677, 2017.
- [42] K. F. El-Nemr, and R. M. Mohamed, "Sorbic acid as friendly curing agent for enhanced properties of ethylene propylene diene monomer rubber using gamma radiation," *Journal of Macromolecular Science, Part A*, vol. 54, no. 10, pp. 711-719, 2017.
- [43] F. K. Liew, S. Hamdan, M. M. Rahman, M. Rusop, J. Lai, Md. F. Hossen, Md. and M. Rahman, "Synthesis and characterization of cellulose from green bamboo by chemical treatment with mechanical process," *Journal of Chemistry*, vol. 2015, no. 212158, pp. 1-6, 2015.
- [44] R. Wittawat, R. Rittipun, and B. Nattaporn, "Development of PLA/EPDM/SiO<sub>2</sub> blended polymer for biodegradable packaging," *Journal of Applied Polymer Science*, vol. 139, no. 48, p. e53239, 2022.
- [45] Z. Qiu, M. Komura, T. Ikehara, and T. Nishi, "DSC and TMDSC study of melting behaviour of poly (butylene succinate) and poly (ethylene succinate)," *Polymer*, vol. 44, no. 26, pp. 7781-7785, 2003.

10 ALAPON, S., et al.

[46] S. Wacharawichanant, P. Sahapaibounkit, U. Saeueng, and S. Thongyai, "Mechanical and thermal properties of polyoxymethylene nanocomposites filled with different nanofillers," *Polymer-Plastics Technology and Engineering*, vol. 53, no. 2, pp. 181-188, 2014.

- [47] T. W. Shyr, H. C. Ko, and H. L. Chen, "Homocrystallization and stereocomplex crystallization behaviors of as-spun and hot-drawn poly(l-lactide)/poly(d-lactide) blended fibers during heating," *Polymers (Basel)*, vol. 11, no. 9, 2019.
- [48] K. F. El-Nemr, M. A. Ali, S. N. Saleh, and A. W. M. El-Naggar, "Mechanical properties of gamma-irradiated styrene-butadiene rubber/acid-treated vermiculite clay/maleic anhydride nanocomposites," *Polymer Engineering & Science*, vol. 59, no. 2, pp. 355-364, 2019.
- [49] A. Gupta, N. Mulchandani, M. Shah, S. Kumar, and V. Katiyar,

- "Functionalized chitosan mediated stereocomplexation of poly (lactic acid): Influence on crystallization, oxygen permeability, wettability and biocompatibility behavior," *Polymer*, vol. 142, pp. 196-208, 2018.
- [50] S. Van Nguyen, and B. K. Lee, "Polyvinyl alcohol/cellulose nanocrystals/alkyl ketene dimer nanocomposite as a novel biodegradable food packing material," *International Journal* of *Biological Macromolecules*, vol. 207, pp. 31-39, 2022.
- [51] S. Saeidlou, M. A. Huneault, H. Li, and C. B. Park, "Poly(lactic acid) crystallization," *Progress in Polymer Science*, vol. 37, no. 12, pp. 1657-1677, 2012.
- [52] H. Urayama, T. Kanamori, and Y. Kimura, "Microstructure and thermomechanical properties of glassy polylactides with different optical purity of the lactate units," *Macromolecular Materials and Engineering*, vol. 286, no. 11, pp. 705-713, 2001.